

Pseudo-five-component synthesis of indolone-3-aminopropenylidene merocyanine dimers and their attenuated aggregation-induced emission

Anna-Lena Elsner, Lukas Biesen, and Thomas J. J. Müller*

Institut für Organische Chemie und Makromolekulare Chemie, Heinrich-Heine-Universität Düsseldorf,
Universitätsstraße 1, 40225 Düsseldorf, Germany
Email: ThomasJ.J.Mueller@uni-duesseldorf.de

Dedicated to Prof. Dr. Lanny L. Liebeskind on the occasion of his 70th birthday

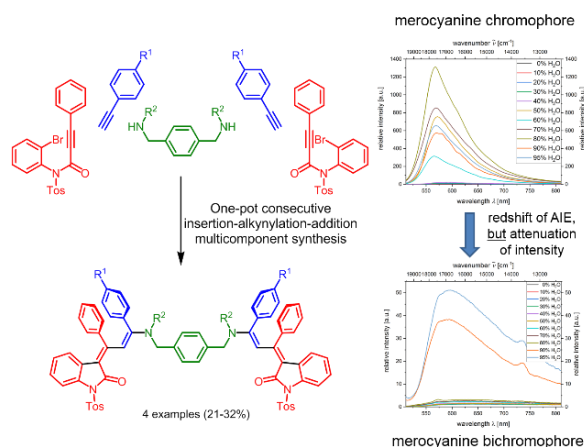
Received 11-16-2020

Accepted 12-17-2020

Published on line 12-23-2020

Abstract

Four indolone-3-aminopropenylidene merocyanine dimers and a reference α -indolonyl- γ -amino merocyanine are readily synthesized in a consecutive multicomponent insertion-alkynylation-addition sequence in a one-pot fashion. The rotational barriers of the terminal amino moieties were estimated by variable temperature NMR measurements and the observed coalescence at room temperature to lie in the same margin as for β -pyrrolidinyloxy enoates. While the mono merocyanine, chosen as a reference, displays the expected 1300 fold increase in emission intensity upon induced aggregation, the merocyanine dimers, although intense in their absorption behavior and redshifted in their emission maxima, only show a 50-60 fold fluorescence increase. The considerable attenuation of emission of the merocyanine dimers in the amorphous solid state supports the finding that unimolecular symmetrical merocyanine dimers of this type are not intensive AIE systems.



Keywords: Absorption, aggregation-induced emission, alkynylation, cross-coupling, copper, indole, merocyanine, palladium

Introduction

Merocyanines,¹⁻⁶ neutral polyenes with terminal +M-donor and –M-acceptor substituents, are highly polarizable π -electron systems with high extinction coefficients that have found application as chromophores in optoelectronics,⁷⁻¹⁰ organic semiconductors,¹¹ and photovoltaics.¹² In addition, the self-assembly of merocyanines in solution represents an elegant approach to nanoscale objects and supramolecular materials.^{13,14} The classical synthesis of merocyanines, as for many polymethine dyes, is governed by conventional aldol or Knoevenagel condensations.^{1, 15-17} In recent years, chromophores, fluorophores and electrophores¹⁸⁻²⁰ with heterocyclic scaffolds have become readily accessible by application of the concepts of multicomponent reactions (MCRs)²¹⁻²⁴ and domino processes.²⁵⁻²⁶ In particular, MCR by catalytic generation of alkynoyl intermediates²⁷ turned out to be an excellent access to fluorophores in a modular one-pot fashion.²⁸ Among fluorescent chromophores, molecules that are nonluminescent in solution but emissive in the solid state, are particularly interesting for materials applications. Indeed, this unusual behavior is strongly correlated with molecular aggregation and, therefore, has been called aggregation-induced emission (AIE), a term coined by Tang and coworkers.²⁹⁻³² Mechanistic aspects of this "light-up upon aggregation" are still under debate. Due to their highly polar nature, merocyanines are predestined for aggregation⁵ and also for AIE phenomena. Indeed, MCR can be well employed for developing modular one-pot syntheses of solid-state emissive merocyanines with AIE properties.³³⁻³⁴ In recent years, we have developed three-component syntheses of indolone-based merocyanines, i.e. α -indolonyl- ω -amino systems **1**, **2**, and **3** (Figure 1),³⁵⁻³⁸ based upon consecutive one-pot insertion-alkynylation-addition sequences.³⁹ Particularly interesting are merocyanines **1** and **2**, which not only show intense solid state fluorescence upon UV excitation, but also distinct AIE characteristics, which have been studied in detail for merocyanines **1** with 3-piperazinyl donors.³⁷ These peculiar donor functionalities also enabled the conceptual extension to four-component insertion-alkynylation-addition-Suzuki syntheses of white-light emissive bichromophores operated by aggregation-induced dual emission.⁴⁰

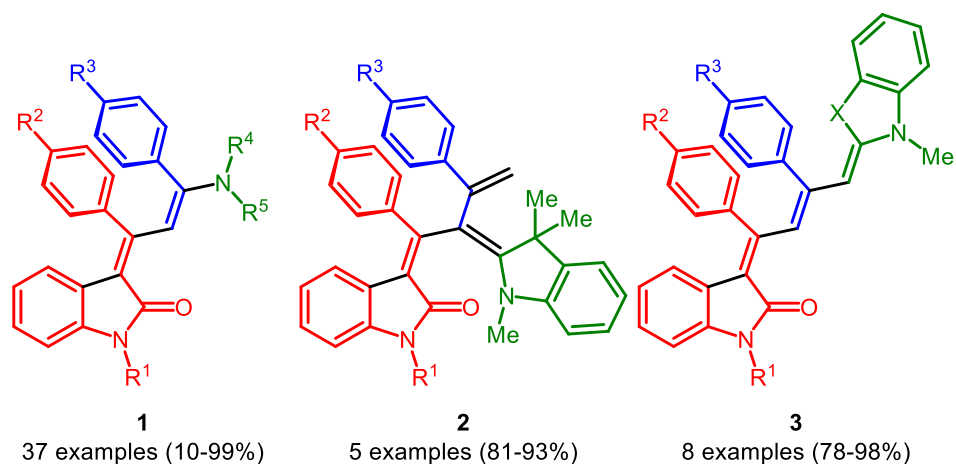


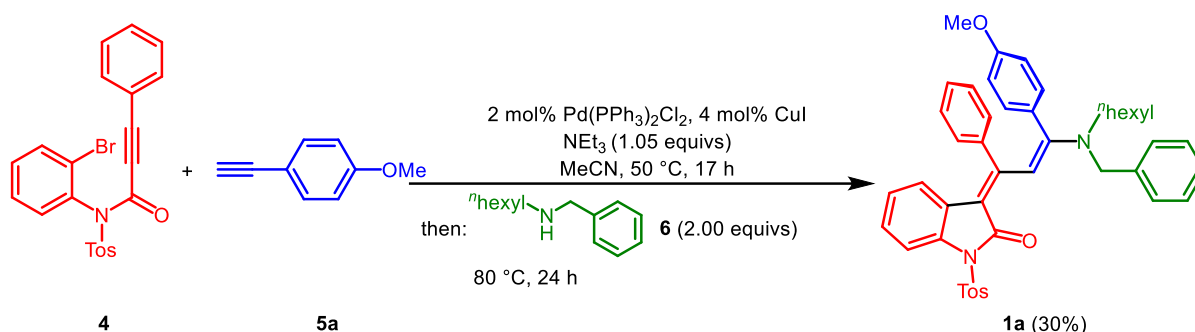
Figure 1. α -Indolonyl- ω -amino merocyanines **1**, **2**, and **3** synthesized by consecutive three-component insertion-alkynylation-addition sequences.

Inspired by dipole-dipole-induced self-organization of merocyanines^{13,14} to dimers and of merocyanine dimers⁴¹⁻⁴⁵ to ordered aggregates, we reasoned that homo-bichromophores of α -indolonyl- ω -amino merocyanines could be interesting models for exploring induced aggregation of merocyanines **1** and ultimately

their fluorescence light up. Herein, we report the synthesis and the AIE behavior of a selected homo-bichromophore.

Results and Discussion

Based upon our previous protocols for the synthesis of 3-piperazinyl propenylidene indolones³⁷ and starting from *N*-tosyl 3-phenyl propynoyl *ortho*-bromo anilide (**4**), and 1-ethynyl-4-methoxybenzene (**5a**), and *N*-benzylhexan-1-amine (**6**) the reference 3-amino propenylidene indolone **1a** was obtained in 30% yield after chromatography on silica gel (Scheme 1).



Scheme 1. Three-component synthesis of model merocyanine **1a**.

Likewise, homo-bichromophores **8** were prepared by insertion-alkynylation-addition sequence starting from *N*-tosyl 3-phenyl propynoyl *ortho*-bromo anilide (**4**), and aryl alkyne **5**, and *N,N'*-(1,4-phenylenebis(methylene))dialkanamines **7** in a 2:2:1 ratio in the sense of a consecutive pseudo five-component reaction. The title compounds **8** were obtained in 21-32% yield after chromatography on silica gel (Scheme 2). Taking into account that six new bonds are formed in a one-pot fashion, the average yield per bond forming step amounts to 77-83%.

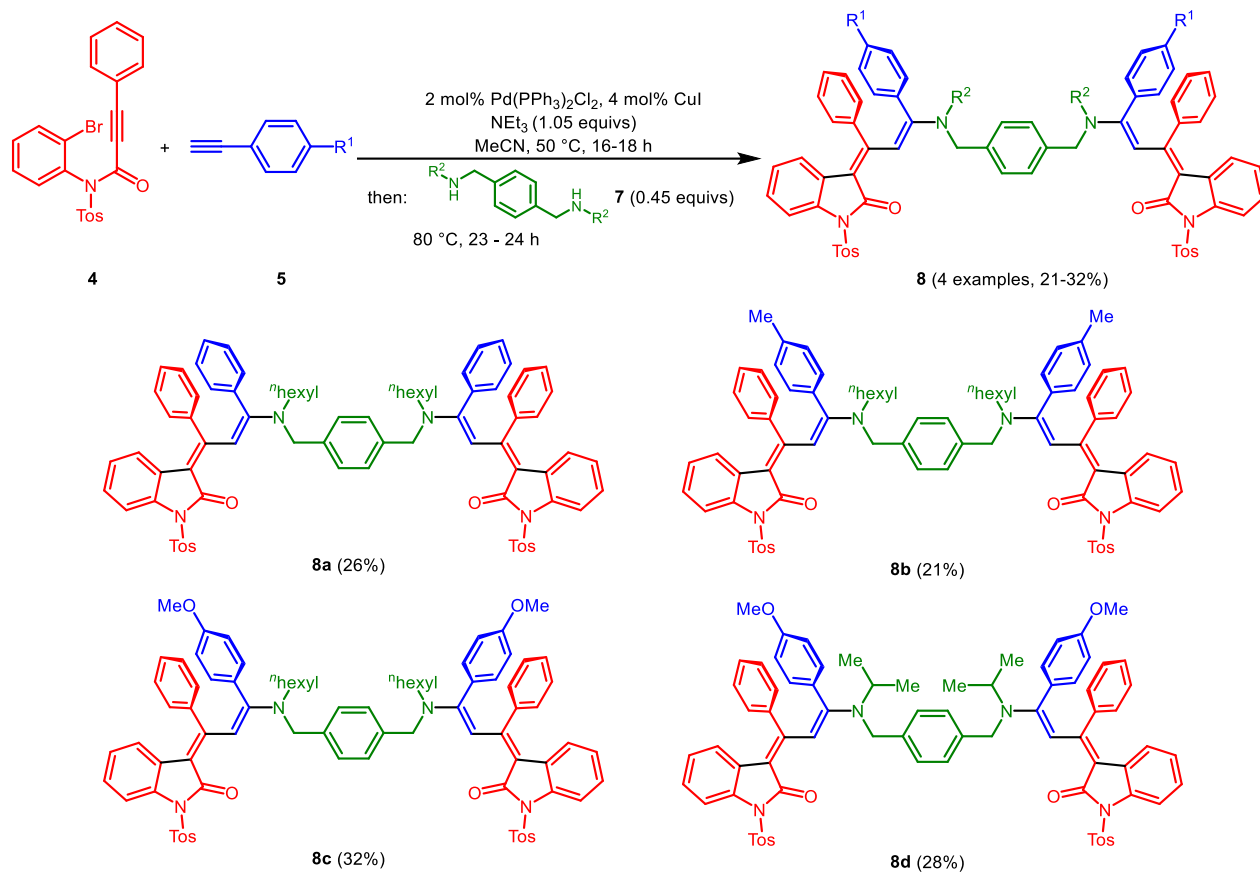
The molecular structures of reference chromophore **1a** and bichromophores **8** were assigned by ¹H and ¹³C NMR spectroscopy and mass spectrometry. As anticipated, for the bichromophores **8** a reduced set of signals is observed, in accordance with the molecular symmetry. Furthermore, it can be deduced as for previously reported α -indolonyl- ω -amino merocyanines **1**, that only a single diastereomer is formed.³⁵

The rotational barrier of the merocyanine C-N-bond can be estimated from the coalescence temperature of the methylene protons adjacent to the nitrogen atom, of both the hexyl chain and the benzyl group. From room temperature proton NMR spectra (see Supporting Information) it can be estimated that the coalescence temperature T_c apparently is around room temperature (293 K) for the reference system **1a** and the three consanguineous bichromophores **8a**, **8b**, and **8c**. Upon increasing the temperature to 323 K, two signals at δ 3.15-3.23 and δ 4.28-4.44 evolve for the *N*-methylene protons of the hexyl side-chain and the benzylic protons. Lowering the temperature to 263 K causes a resolution into two sets of diastereotopic signals for these protons. These pairs of signals merge at the coalescence temperature T_c . The rate constant for the internal dynamic process, i.e. the C-N-bond rotation, is described for both signals by equation (1).

$$k_{T_c} = \frac{\pi}{\sqrt{2}} |v_A - v_B| \quad (1)$$

ν = frequency in Hz.

Insertion of equation (1) into the Eyring equation, and rearranging, gives the free enthalpy of activation ΔG^\ddagger (equation (2)) for the examined process.



Scheme 2. Consecutive pseudo five-component synthesis of homo-bichromophores **8** by insertion-alkynylation-addition sequence.

$$\Delta G^\ddagger = RT_c \cdot \ln \frac{RT_c \sqrt{2}}{\pi \cdot N_A \cdot h |v_A - v_B|} \quad (2)$$

R = gas constant, T_c = coalescence temperature in K.

Insertion of constants in equation (2) finally gives ΔG^\ddagger as function of T_c and $\Delta \nu$ (equation (3)).

$$\Delta G^\ddagger = 19.1 \cdot 10^{-3} \cdot T_c (9.97 + \log T_c - \log |v_A - v_B|) \quad (3)$$

For a coalescence temperature T_c of 293 K (20 °C) and the frequency differences $\Delta \nu$ the rotational barriers of the merocyanine C-N-bonds are estimated from ΔG^\ddagger (Table 1).

Table 1. Rotational barriers of the merocyanine C-N-bonds $\Delta G^\ddagger(293\text{ K})$ at a coalescence temperature $T_c = 293\text{ K}$ of reference system **1a** and the three consanguineous bichromophores **8a**, **8b**, and **8c** and the resolved diastereotopic sets of *N*-methylene and *N*-benzyl protons determined at 263 K from the proton NMR spectra

Compound	$\delta_A - \delta_B$	$ v_A - v_B $ [Hz]	$\Delta G^\ddagger(293\text{ K})$ [kJ/mol]
1a (<i>N</i> -methylene)	3.42 - 2.82 = 0.6	360	55.3
1a (<i>N</i> -benzyl)	4.72 - 4.08 = 0.64	384	55.1
8a (<i>N</i> -methylene)	3.46 - 2.84 = 0.62	372	55.2
8a (<i>N</i> -benzyl)	4.78 - 4.04 = 0.74	444	54.8
8b (<i>N</i> -methylene)	3.44 - 2.88 = 0.56	336	55.5
8b (<i>N</i> -benzyl)	4.77 - 4.10 = 0.67	402	55.0
8c (<i>N</i> -methylene)	3.55 - 2.90 = 0.65	390	55.1
8c (<i>N</i> -benzyl)	4.60 - 4.04 = 0.56	336	55.5

The average of the free enthalpy of activation ΔG^\ddagger can be determined for the merocyanines **1a** and **8a**, **8b**, and **8c** in a narrow range of 55.2 ± 0.2 kJ/mol. This rotational barrier is relatively low and lies at a comparable magnitude as recently determined for ethyl β -pyrrolidino enoates.⁴⁶

The reference chromophore **1a** is an orange solid that luminesces under a hand-held UV lamp, in agreement with the photophysical behavior of many other α -indolonyl- γ -amino merocyanines **1**.³⁵⁻³⁸ As previously shown for merocyanines **1** with 3-piperazinyl donors,³⁷ we first recorded the UV/vis spectrum of reference chromophore **1a** (Figure 1), showing an intense merocyanine typical broad absorption band at 490 nm with an absorption coefficient of $43500\text{ L}\cdot\text{mol}^{-1}\cdot\text{cm}^{-1}$. The AIE measurements in 1,4-dioxane/water mixtures with increasing water fraction produce an emission signal upon inducing aggregation that is visible to the naked eye (Figure 2) and reaches a maximum of 568 nm at a water fraction of 80% (Figure 3).

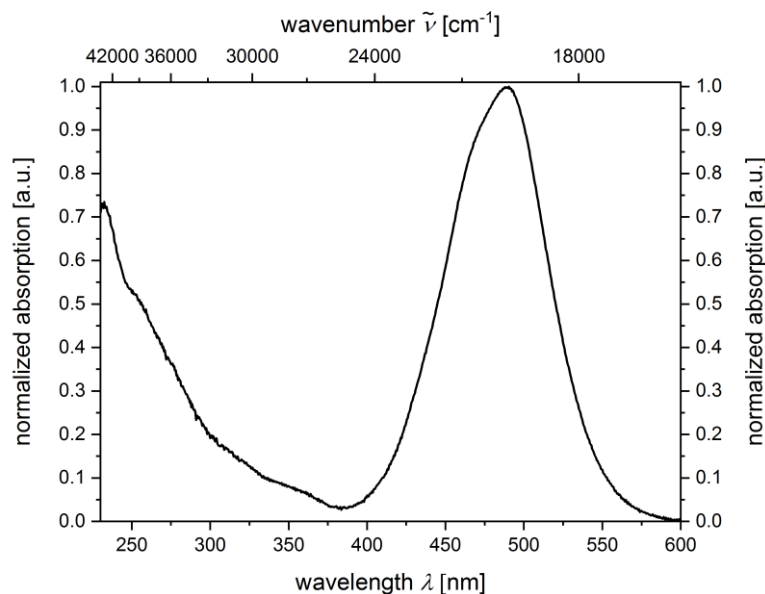


Figure 2. Absorption spectrum of compound **1a** in dichloromethane (recorded at $T = 298\text{ K}$, $c(\mathbf{1a}) = 10^{-5}\text{ M}$).

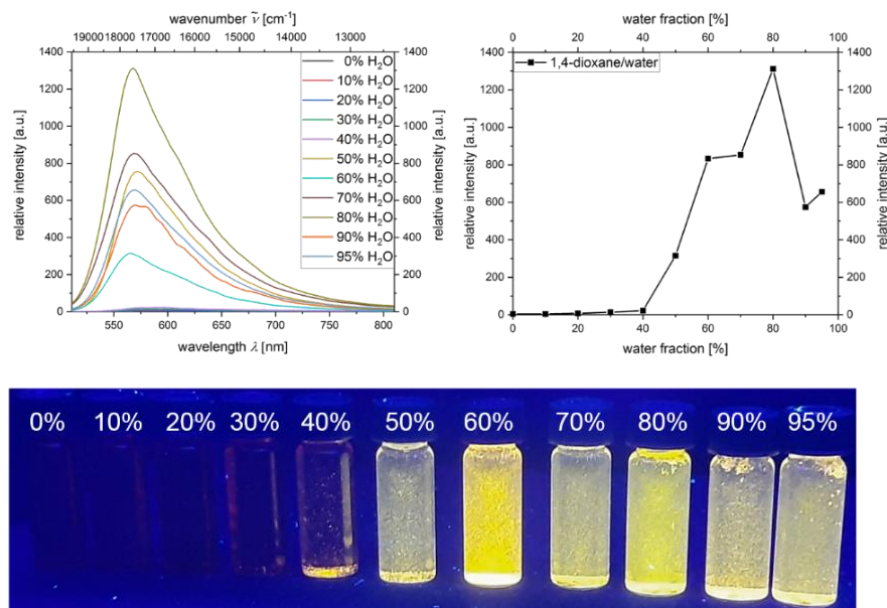


Figure 3. Emission spectra of compound **1a** in 1,4-dioxane/water mixtures upon increasing water content (top, left) and intensity as a function of the water fraction of the 1,4-dioxane/water mixtures content (top, right) (recorded at $T = 298\text{ K}$, $c(\mathbf{1a}) = 10^{-4}\text{ M}$, $\lambda_{exc}(\mathbf{1a}) = 490\text{ nm}$) and visual impression of the AIE (bottom) upon excitation with a handheld UV-lamp ($\lambda_{exc} = 365\text{ nm}$).

As would be expected, the homo-bichromophores **8** display superimposing UV/vis spectra in dichloromethane with broad intense longest wavelength absorption maxima λ_{max} at 490-491 nm with absorption coefficients of 74600 (**8b**), 73300 (**8c**) and 63300 $\text{L}\cdot\text{mol}^{-1}\cdot\text{cm}^{-1}$ (**8d**) (Figure 4), indicating that despite variation of substituents R^1 and R^2 , the chromophore is essentially the same and that in the electronic ground state, reflected by UV/vis absorptions, the two constituting merocyanine moieties are essentially electronically decoupled.

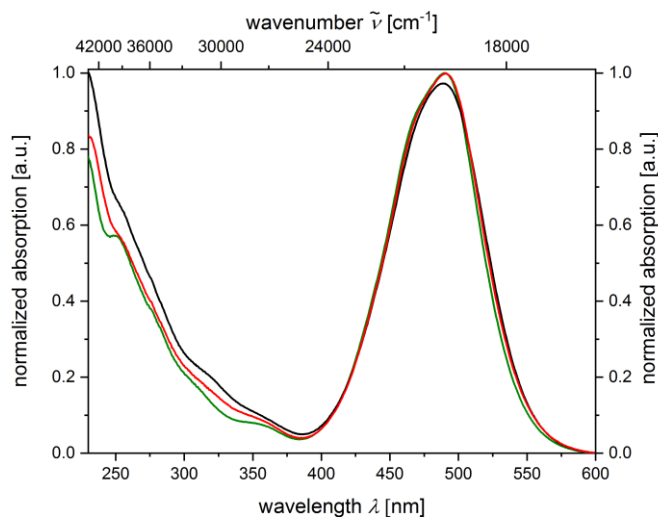


Figure 4. Absorption spectra of compounds **8b** (green), **8c** (red) and **8d** (black) in dichloromethane (recorded at $T = 298\text{ K}$, $c(\mathbf{8}) = 10^{-5}\text{ M}$).

In place of homo-bichromophores **8** the AIE measurements were performed for bichromophore **8d** (Figure 5, however, in two polarity opposing solvent mixtures, i.e. 1,4-dioxane/water mixtures with increasing content of water (Figure 5, left) and dichloromethane/cyclohexane mixtures with increasing content of cyclohexane (Figure 5, right). While the former produce a 60-fold increase of the emission signal upon inducing aggregation with a maximum at 613 nm at a water fraction of 80% (Figure 4, left, bottom), the latter leads to a 50-fold emission increase of the band at 597 nm for a 95% fraction of cyclohexane (Figure 4, right, bottom). In comparison to the reference chromophore **1a** the AIE of bichromophore **8d** clearly redshifted in both solvent mixtures, indicating that the intramolecular merocyanine-merocyanine interaction obviously causes a lowering in the excited state energies in the bichromophore aggregates. However, in comparison to the reference chromophore **1a** (1300-fold) the AIE enhancement of bichromophore **8d** in both solvent systems is with 50- to 60-fold significantly lower. Therefore, it can be assumed that the *anti*-parallel molecular orientation of the merocyanine units in the aggregates of bichromophore **8d** largely overcompensates for the AIE effect gained in the monochromophore system **1a**. This effect is also visible to the naked eye for the amorphous powders under a handheld UV lamp (Figure 6). While merocyanine **1a** brightly shines upon UV excitation, homo-bichromophore **8d** is only very weakly emissive.

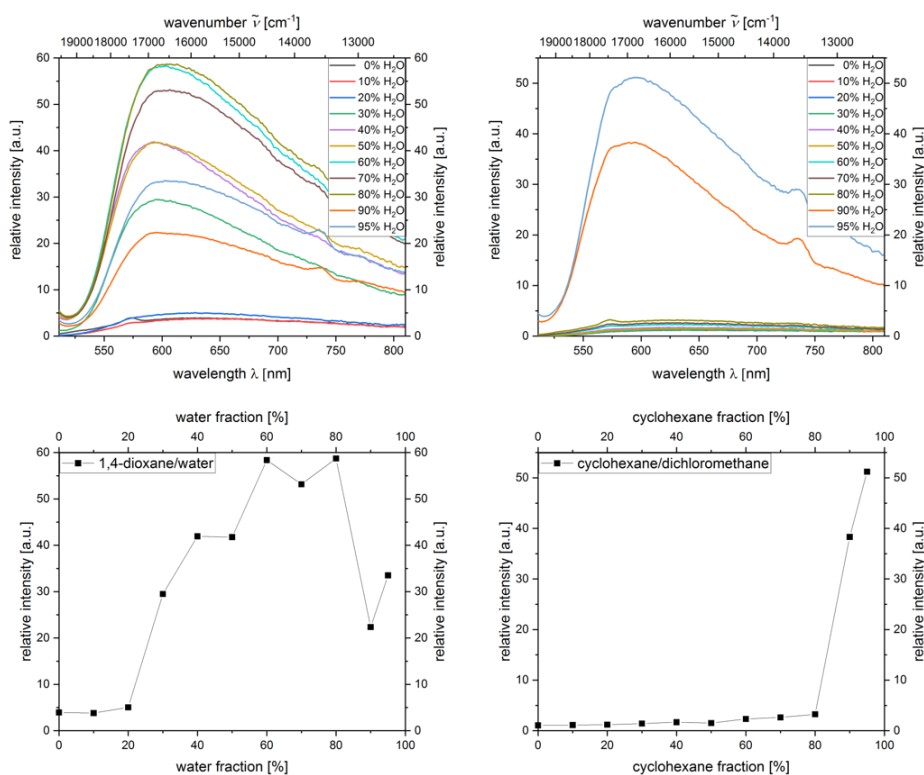


Figure 5. Emission spectra of compound **8d** in 1,4-dioxane/water mixtures (top, left) and dichloromethane/cyclohexane mixtures (top, right) upon increasing content of water and cyclohexane, respectively. Emission intensity as a function of the water fraction of the 1,4-dioxane/water mixtures (bottom, left) and as a function of the cyclohexane fraction of the dichloromethane/cyclohexane mixtures (bottom, right) (recorded at $T = 298$ K, $c(\mathbf{8d}) = 10^{-4}$ M, $\lambda_{exc}(\mathbf{8d}) = 490$ nm).

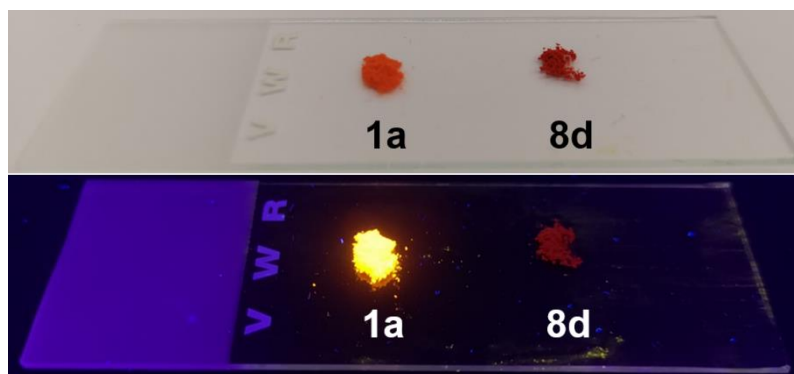


Figure 6. Amorphous powders of merocyanine **1a** and homo-bichromophore **8d** on a microscope slide under daylight (top) and under UV light upon excitation with a handheld UV-lamp ($\lambda_{\text{exc}} = 365 \text{ nm}$) (bottom).

Conclusions

The synthetic one-pot insertion-alkynylation-addition concept of the three-component synthesis of α -indolonyl- γ -amino merocyanines can be readily expanded to the formation of merocyanine dimers in the sense of a pseudo-five-component fashion. While the absorption characteristics of these homo-bichromophores behave essentially in an additive manner, as expected for non-interacting multichromophores in the electronic ground state, the excited state behavior deviates significantly from the reference monomerocyanine. While the latter displays a significant enhancement of emission upon induced aggregation in solvent mixtures, the model homo-bichromophore only reveals a very modest increase of emission, although with distinct redshift. This indicates that the monomerocyanine typical gain of fluorescence in the series of α -indolonyl- γ -amino merocyanines is significantly attenuated as a consequence of a potential symmetrical anti-parallel alignment of the merocyanines upon aggregation. This finding also holds true in the solid state, as supported by comparison of reference monomerocyanine with homo-bichromophore under the handheld UV lamp. As a consequence, for the design of unimolecular multichromophore AIE systems, either breaking the structural or electronic symmetry might give a trade-off. Just very recently we could show that α -indolonyl- γ -amino merocyanines are well-suited for designing donor-acceptor bichromophores showing aggregation induced dual emission (AIDE) operated by partial energy transfer.⁴⁰ Further studies to enhance multichromophore AIE by donor-acceptor patterns are currently under investigation.

Experimental Section

(E)-3-((E)-3-(Benzyl(hexyl)amino)-3-(4-methoxyphenyl)-1-phenylallylidene)-1-tosylindolin-2-one (1a). In an oven-dried Schlenk tube with magnetic stir bar, Pd(PPh₃)₂Cl₂ (6.79 mg, 0.01 mmol, 2 mol%) and CuI (3.70 mg, 0.02 mmol, 4 mol%) were placed under nitrogen and dry acetonitrile (3 mL) was added. Amide **4** (227 mg, 0.50 mmol) was added to the suspension, which dissolved at 50 °C (oil bath) after 4 min. After cooling to room temp dry triethylamine (52.9 mg, 0.52 mmol) was added and the mixture was stirred at rt for 20 min. Then, 1-ethynyl-4-methoxybenzene (**5a**) (73.0 mg, 0.55 mmol) was added to the reaction mixture and stirring at rt was continued for 10 min before the mixture was heated at 50 °C (oil bath) for 17 h. After cooling to rt, *N*-benzyl hexan-1-amine (**6**) (191 mg, 1.00 mmol) was added and the reaction mixture was stirred at 80 °C (oil bath) for

24 h. After cooling to rt, CH₂Cl₂ (10 mL) was added and the organic phase was extracted with saturated aq NH₄Cl solution (10 mL). The aq layer was extracted with CH₂Cl₂ (3 x 10 mL). The combined organic layers were washed with brine (20 mL), dried (anhydrous MgSO₄) and the organic solvents were removed under reduced pressure. The residue was adsorbed on Celite® and purified by flash chromatography on silica gel (*n*-hexane/Me₂CO, 15:1) and after crystallization from hexane/Me₂CO, compound **1a** (107 mg, 31%) was isolated as an orange fluorescent solid, mp 118 °C, R_f (*n*-hexane/EtOAc, 6:1) = 0.38.

¹H NMR (600 MHz, CDCl₃, *T* = 293 K), δ = 0.86 (t, ³*J* = 6.4 Hz, 3 H), 1.24–1.35 (m, 6 H), 1.58–1.60 (m, 1 H), 2.42 (s, 3 H), 3.29 (m, 1 H), 3.69 (s, 3 H), 5.28 (d, ³*J* = 8.0 Hz, 1 H), 6.42 (d, ³*J* = 8.3 Hz, 1 H), 6.49 (t, ³*J* = 7.7 Hz, 1 H), 6.63 (s, 1 H), 6.73 (d, ³*J* = 8.2 Hz, 2 H), 6.90 (d, ³*J* = 7.6 Hz, 1 H), 6.95 (d, ³*J* = 7.6 Hz, 2 H), 7.02 (d, ³*J* = 7.4 Hz, 2 H), 7.19 (m, 2 H), 7.26–7.34 (m, 5 H), 7.59 (m, 1 H), 7.87 (d, ³*J* = 8.2 Hz, 2 H), 8.05 (d, ³*J* = 8.2 Hz, 2 H).^a ¹³C NMR (150 MHz, CDCl₃) δ = 14.2 (CH₃), 21.8 (CH₃), 22.7 (CH₂), 26.62 (CH₂), 26.63 (CH₂), 31.5 (CH₂), 54.7 (CH₂), 55.4 (CH₃), 109.2 (CH), 112.4 (CH), 113.4 (CH), 120.6 (CH), 122.8 (CH), 124.4 (CH), 126.7 (CH), 127.2 (C_{quat}), 127.6 (CH), 127.8 (CH), 128.0 (CH), 128.8 (CH), 129.1 (C_{quat}), 129.5 (CH), 130.4 (C_{quat}), 131.4 (CH), 135.0 (CH), 137.0 (CH), 137.4 (C_{quat}), 140.5 (C_{quat}), 144.4 (C_{quat}), 159.6 (C_{quat}), 159.7 (C_{quat}), 164.5 (C_{quat}), 165.6 (C_{quat}).^b MALDI-TOF: *m/z* = 697.3 [M – H]⁺, 543.3 [M – Tos]⁺. IR (neat): $\tilde{\nu}$ [cm⁻¹] = 2957 (w), 2924 (w), 2859 (w), 1659 (m), 1611 (w), 1595 (w), 1503 (m), 1491 (w), 1470 (m), 1452 (w), 1433 (w), 1389 (w), 1369 (w), 1341 (m), 1321 (w), 1292 (m), 1248 (m), 1223 (w), 1190 (m), 1165 (m), 1144 (w), 1119 (w), 1067 (s), 1047 (w), 1026 (m), 999 (m), 959 (m), 935 (w), 916 (m), 901 (m), 876 (m), 827 (m), 808 (m), 777 (m), 762 (m), 743 (s), 712 (w), 689 (m). Anal. calcd. for C₄₄H₄₄N₂O₄S (696.9): C 75.83, H 6.36, N 4.02, S 4.60; Found: C 76.10, H 6.51, N 3.87, S 4.36. UV/Vis: λ_{max} [nm] (ϵ [L·mol⁻¹·cm⁻¹]) = 489.5 (43500).

General procedure (GP) for the pseudo five-component synthesis of merocyanine dimers **8.** In an oven-dried Schlenk tube with magnetic stir bar, Pd(PPh₃)₂Cl₂ (7.0 mg, 10 μmol, 2 mol%) and CuI (3.8 mg, 20 μmol, 4 mol%) were placed under N₂ and dry MeCN (3 mL) was added. Amide **4** (227 mg, 0.50 mmol) was added to the suspension, which dissolved at 50 °C (oil bath) after 4 min. After cooling to rt, alkyne **5** (0.55 mmol) and dry Et₃N (52.9 mg, 0.52 mmol) were added to the reaction mixture, which turned from yellow to brown (for experimental details, see Table 2). Then the mixture was heated at 50 °C (oil bath) for 16-18 h. After cooling to rt, compound **7** (0.23 mmol) was added and the reaction mixture turned red. The reaction mixture was stirred at 80 °C (oil bath) for 22-24 h and the product precipitated from solution. After cooling to rt, CH₂Cl₂ (20 mL) was added and the organic phase was extracted with saturated aq NH₄Cl solution (15 mL). The aq layer was extracted with CH₂Cl₂ (3 x 10 mL). The combined organic layers were washed with brine (20 mL), dried (anhydrous MgSO₄) and the organic solvents were removed under reduced pressure. The residue was adsorbed on Celite® and purified by flash chromatography on silica gel (*n*-hexane/Me₂CO). For removing solvent inclusions, the purified products were dissolved in a minimum of CH₂Cl₂, *n*-hexane was added to the solution for precipitation and placed in the ultrasound bath for 10 min. After decantation the residual solvents were removed under reduced pressure and the pure products **8** were obtained as orange to red solids.

Table 2. Experimental details of the pseudo-five-component synthesis of merocyanine dimers **8**

Entry	Alkyne 5	Diamine 7	Merocyanine dimer 8
1	56.3 mg (0.55 mmol) of 5b	68.7 mg (0.23 mmol) of 7a	73.5 mg (26%) of 8a
2	64.1 mg (0.55 mmol) of 5c	68.6 mg (0.23 mmol) of 7a	61.8 mg (21%) of 8b
3	73.0 mg (0.55 mmol) of 5a	68.1 mg (0.22 mmol) of 7a	95.1 mg (32%) of 8c
4	73.1 mg (0.55 mmol) of 5a	49.1 mg (0.22 mmol) of 7b	78.7 mg (28%) of 8d

(3E,3'E)-3,3'-((2E,2'E)-((1,4-Phenylenebis(methylene))bis(hexylazanediy))bis(1,3-diphenylprop-2-en-3-yl-1-ylidene))bis(1-tosylindolin-2-one) (8a). According to the GP and after chromatography on silica gel (*n*-hexane/Me₂CO, 15:1 to 10:1), precipitation from CH₂Cl₂/*n*-hexane and ultrasonication compound **8a** (73.5 mg, 26%) was isolated as an orange solid, mp 219 °C, *R_f* (*n*-hexane/Me₂CO, 3:1) = 0.18.

¹H NMR (600 MHz, CDCl₃, *T* = 293 K), δ = 0.75–0.89 (m, 6 H), 1.17–1.28 (m, 12 H), 1.57 (m, 4 H), 2.40 (s, 6 H), 5.25 (d, ³*J* = 7.9 Hz, 2 H), 6.48 (t, ³*J* = 7.7 Hz, 2 H), 6.61 (s, 2 H), 6.80 (m, 4 H), 6.87–6.94 (m, 10 H), 6.96–7.00 (m, 6 H), 7.15 (m, 4 H), 7.29 (m, 4 H), 7.62 (m, 2 H), 7.86 (m, 2 H), 8.05 (d, ³*J* = 8.0 Hz, 4 H).^c ¹³C NMR (150 MHz, CDCl₃) δ = 14.0 (CH₃), 21.7 (CH₃), 22.5 (CH₂), 26.45 (CH₂), 26.47 (CH₂), 31.35 (CH₂), 31.43 (CH₂), 54.2 (CH₂), 109.5 (C_{quat}), 112.3 (CH), 120.6 (CH), 122.7 (CH), 124.5 (CH), 126.4 (C_{quat}), 127.2 (CH), 127.5 (CH), 127.7 (CH), 127.8 (CH), 128.0 (CH), 128.9 (CH), 129.4 (CH), 129.9 (CH), 134.9 (C_{quat}), 136.1 (C_{quat}), 136.2 (C_{quat}), 136.8 (C_{quat}), 140.0 (C_{quat}), 144.4 (C_{quat}), 159.1 (C_{quat}), 164.0 (C_{quat}), 165.5 (C_{quat}).^d MALDI-TOF: *m/z* = 1257.56 [M + 2 H]⁺, 1255.58 [M + H]⁺, 1101.54 [M + 2 H – Tos]⁺, 679.32 [C₄₄H₄₃N₂O₃S]⁺. IR (neat): $\tilde{\nu}$ [cm⁻¹] = 2926 (w), 2855 (w), 1682 (m), 1597 (m), 1506 (s), 1487 (s), 1456 (m), 1435 (w), 1418 (m), 1364 (m), 1346 (m), 1319 (m), 1296 (m), 1242 (m), 1227 (w), 1200 (m), 1157 (s), 1119 (w), 1092 (w), 1070 (s), 1043 (w), 1001 (m), 995 (w), 962 (m), 934 (m), 920 (w), 908 (w), 885 (w), 814 (m), 766 (m), 741 (m), 733 (m), 713 (w), 700 (m), 689 (m), 658 (m), 644 (m), 623 (w), 611 (m). HRMS (ESI) *m/z* (%) calcd. for [C₈₀H₇₈N₄O₆S₂ + H]⁺: 1255.5436 (100), 1256.5469 (87), 1257.5394 (9), 1257.5503 (37), 1258.5427 (8), 1258.5536 (10), 1259.5461 (2); Found: 1254.5303 (13),^e 1255.5421 (100), 1256.5455 (80), 1257.5469 (40), 1258.5475 (17), 1259.5485 (7).

(3E,3'E)-3,3'-((2E,2'E)-((1,4-Phenylenebis(methylene))bis(hexylazanediy))bis(1-phenyl-3-(*p*-tolyl)prop-2-en-3-yl-1-ylidene))bis(1-tosylindolin-2-one) (8b). According to the GP and after chromatography on silica gel (*n*-hexane/Me₂CO, 12:1 to 10:1), precipitation from CH₂Cl₂/*n*-hexane and ultrasonication compound **8b** (61.8 mg, 21%) was isolated as a red orange solid, mp 222 °C, *R_f* (*n*-hexane/Me₂CO, 3:1) = 0.27.

¹H NMR (600 MHz, CDCl₃, *T* = 293 K), δ = 0.83–0.88 (m, 6 H), 1.12–1.34 (m, 12 H), 1.57 (s, 4 H), 2.15 (s, 6 H), 2.40 (s, 6 H), 5.24 (d, ³*J* = 7.9 Hz, 2 H), 6.48 (t, ³*J* = 7.7 Hz, 2 H), 6.67–6.69 (m, 8 H), 6.90 (m, 6 H), 7.00–7.01 (m, 4 H), 7.26–7.29 (m, 10 H), 7.62–7.72 (m, 2 H), 7.86 (m, 2 H), 8.04 (d, ³*J* = 8.5 Hz, 4 H).^f ¹³C NMR (150 MHz, CDCl₃) δ = 14.2 (CH₃), 21.3 (CH₃), 21.8 (CH₃), 22.7 (CH₂), 26.6 (CH₂), 31.49 (CH₂), 31.53 (CH₂), 31.58 (CH₂), 31.6 (CH₂), 109.2 (C_{quat}), 112.4 (CH), 120.7 (CH), 122.8 (CH), 124.4 (CH), 126.7 (C_{quat}), 127.0 (CH), 127.2 (CH), 127.96 (CH), 128.0 (CH), 128.5 (CH), 128.4 (CH), 129.1 (CH), 129.5 (C_{quat}), 130.4 (C_{quat}), 135.0 (C_{quat}), 137.0 (C_{quat}), 138.3 (C_{quat}), 140.3 (C_{quat}), 144.5 (C_{quat}), 159.6 (C_{quat}), 164.8 (C_{quat}), 165.7 (C_{quat}).^g MALDI-TOF: *m/z* = 1283.63 [M + H]⁺, 1129.62 [M + 2H – Tos]⁺, 693.38 [C₄₅H₄₅N₂O₃S]⁺. IR (neat), $\tilde{\nu}$ [cm⁻¹] = 2953 (w), 2920 (w), 2851 (w), 1692 (m), 1597 (w), 1501 (s), 1491 (m), 1452 (m), 1431 (w), 1414 (m), 1362 (m), 1344 (m), 1319 (m), 1296 (m), 1279 (w), 1242 (m), 1198 (m), 1159 (m), 1117 (w), 1092 (w), 1065 (s), 1042 (m), 1018 (m), 993 (m), 976 (w), 959 (m), 945 (w), 624 (m), 905 (m), 812 (m), 799 (m), 777 (m), 735 (m), 687 (s), 664 (s), 640 (m), 613 (m). Anal. calcd. for C₈₂H₈₂N₄O₆S₂ (1284.7): C 76.72, H 6.44, N 4.36, S 4.99; Found: C 76.55, H 6.45, N 4.18, S 4.70. UV/Vis: λ_{max} [nm] (ϵ [L·mol⁻¹·cm⁻¹]) = 490.1 (74600).

(3E,3'E)-3,3'-((2E,2'E)-((1,4-Phenylenebis(methylene))bis(hexylazanediy))bis(3-(4-methoxyphenyl)-1-phenylprop-2-en-3-yl-1-ylidene))bis(1-tosylindolin-2-one) (8c). According to the GP and after chromatography on silica gel (*n*-hexane/Me₂CO, 5:1 to 3:1 + 3% NEt₃), precipitation from CH₂Cl₂/*n*-hexane and ultrasonication compound **8c** (95.1 mg, 32%) was isolated as a red solid, mp 199 °C, *R_f* (*n*-hexane/Me₂CO 3:1) = 0.22.

¹H NMR (600 MHz, CDCl₃, *T* = 293 K), δ = 0.82–0.90 (m, 6 H), 1.05–1.36 (m, 12 H), 1.50–1.77 (m, 4 H), 2.40 (s, 6 H), 3.67 (s, 6 H), 5.28 (d, ³*J* = 8.0 Hz, 2 H), 6.42 (d, ³*J* = 8.1 Hz, 4 H), 6.46–6.53 (m, 2 H), 6.63 (s, 4 H), 6.70–6.78 (m, 4 H), 6.88–7.03 (m, 8 H), 7.08–7.22 (m, 4 H), 7.28 (d, ³*J* = 8.4 Hz, 4 H), 7.58 (s, 2 H), 7.86 (d, ³*J* = 8.1 Hz, 2 H), 8.01–8.09 (m, 4 H).^h ¹³C NMR (150 MHz, CDCl₃) δ = 14.0 (CH₃), 21.6 (CH₃), 22.3 (CH₂), 22.4 (CH₂), 22.5 (CH₂),

26.3 (CH₂), 31.3 (CH₂), 55.2 (CH₃), 109.1 (C_{quat}), 112.2 (CH), 113.2 (CH), 120.4 (CH), 122.6 (CH), 124.3 (CH), 126.5 (C_{quat}), 127.1 (CH), 127.7 (CH), 127.9 (CH), 128.4 (C_{quat}), 128.9 (CH), 129.3 (CH), 131.3 (CH), 134.8 (C_{quat}), 136.5 (C_{quat}), 136.8 (C_{quat}), 140.2 (C_{quat}), 144.3 (C_{quat}), 159.5 (C_{quat}), 164.3 (C_{quat}), 165.5 (C_{quat}).ⁱ MALDI-TOF: m/z = 1315.59 [M + H]⁺, 1313.57 [M – H]⁺, 1161.57 [C₇₅H₇₇N₄O₆S]⁺, 352.43 [C₂₄H₁₈NO₂]⁺. IR (neat), $\tilde{\nu}$ [cm⁻¹] = 3040 (w), 2990 (w), 2961 (w), 2924 (w), 2901 (w), 2886 (w), 2866 (w), 1684 (m), 1609 (w), 1595 (w), 1545 (w), 1499 (s), 1485 (m), 1458 (w), 1441 (m), 1416 (m), 1379 (w), 1364 (m), 1341 (w), 1317 (w), 1294 (m), 1281 (w), 1246 (m), 1242 (w), 1227 (w), 1202 (m), 1175 (m), 1161 (m), 1115 (w), 1067 (s), 1042 (w), 1028 (w), 993 (w), 964 (w), 937 (m), 907 (w), 887 (w), 831 (m), 804 (m), 787 (w), 775 (w), 737 (m), 704 (m), 687 (m), 660 (m), 642 (m). HRMS (ESI) calcd. for [C₈₂H₈₂N₄O₈S₂ + H]⁺: 1315.5647; Found: 1315.5634. UV/Vis: λ_{max} [nm] (ϵ [L·mol⁻¹·cm⁻¹]) = 490.5 (73300).

(3E,3'E)-3,3'-((2E,2'E)-((1,4-Phenylenebis(methylene))bis(isopropylazanediyl))bis(3-(4-methoxyphenyl)-1-phenylprop-2-en-3-yl-1-ylidene))bis(1-tosylindolin-2-one) (8d). According to the GP and after chromatography on silica gel (*n*-hexane/Me₂CO, 20:1 to 8:1), precipitation from CH₂Cl₂/*n*-hexane and ultrasonication compound **8d** (78.7 mg, 28%) was isolated as a red solid, mp 267 °C, *R_f* (*n*-hexane/Me₂CO, 2:1) = 0.43.

¹H NMR (600 MHz, CDCl₃, *T* = 293 K), δ = 1.12 (d, ³*J* = 6.6 Hz, 12 H), 1.26 (s, 2 H), 2.43 (s, 6 H), 3.67 (s, 6 H), 4.56 (br, 4 H), 5.25 (d, ³*J* = 7.9 Hz, 2 H), 6.27 (s, 4 H), 6.42 (t, ³*J* = 7.2 Hz, 6 H), 6.68–6.81 (m, 8 H), 6.81–6.91 (m, 4 H), 7.27–7.42 (m, 10 H), 7.82 (d, ³*J* = 8.2 Hz, 2 H), 8.01–8.12 (m, 4 H). ¹³C NMR (150 MHz, CDCl₃) δ = 19.0 (CH₃), 21.2 (CH₃), 22.0 (CH), 55.6 (CH₃), 67.5 (CH₂), 100.3 (C_{quat}), 112.6 (CH), 113.7 (CH), 120.9 (CH), 123.0 (CH), 124.7 (CH), 126.7 (C_{quat}), 127.37 (CH), 127.42 (CH), 128.06 (CH), 128.10 (CH), 129.2 (CH), 129.9 (CH), 130.6 (C_{quat}), 131.35 (CH), 131.40 (C_{quat}), 135.2 (C_{quat}), 137.2 (C_{quat}), 140.5 (C_{quat}), 144.8 (C_{quat}), 147.1 (C_{quat}), 160.1 (C_{quat}), 165.8 (C_{quat}).^j MALDI-TOF: m/z = 1247.48 [M + O]⁺, 1231.48 [M + H]⁺, 1077.47 [M + 2H – Tos]⁺, 876.38 [C₅₄H₅₆N₃O₆S]⁺, 742.35 [C₄₅H₄₈N₃O₅S]⁺, 667.29 [C₄₂H₃₉N₂O₄S]⁺. IR (neat), $\tilde{\nu}$ [cm⁻¹] = 1682 (m), 1609 (m), 1597 (m), 1485 (m), 1456 (m), 1445 (w), 1422 (w), 1418 (w), 1383 (w), 1358 (m), 1296 (m), 1267 (s), 1246 (s), 1204 (w), 1167 (s), 1125 (m), 1111 (w), 1094 (w), 1067 (s), 1043 (m), 1026 (w), 1018 (m), 997 (m), 976 (w), 962 (m), 934 (w), 912 (w), 905 (w), 845 (w), 829 (s), 814 (w), 800 (w), 777 (m), 741 (m), 733 (w), 714 (w), 704 (m), 689 (m), 664 (m). HRMS (ESI) calcd. for [C₇₆H₇₀N₄O₈S₂ + H]⁺: 1231.4708 (100), 1232.4741 (82), 1233.4666 (9), 1233.4775 (33), 1234.4699 (7), 1234.4808 (9), 1235.4733 (3); Found: 1230.4573 (15),^k 1231.4688 (100), 1232.4723 (81), 1233.4734 (42), 1234.4744 (15), 1235.4753 (4). UV/Vis: λ_{max} [nm] (ϵ [L·mol⁻¹·cm⁻¹]) = 488.7 (63300).

^a The two methylene groups adjacent to the amino nitrogen atom coalesce; at 323 K two broad signals at δ 3.16 and 4.32 form, at 263 K the methylene protons resolve into four diastereotopic signals at δ 2.82 and 3.42, and δ 4.08 and 4.72.

^b A methylene and two quaternary signals superimpose with other signals.

^c The two methylene groups of adjacent to the amino nitrogen atom coalesce; at 323 K two broad signals at δ 3.15 and 4.28 form, at 263 K the methylene protons resolve into four diastereotopic signals at δ 2.84 and 3.46, and δ 4.04 and 4.78.

^d Two methine signals superimpose with other signals.

^e Corresponds to [M]⁺ calcd. m/z = 1254.5363.

^f The two methylene groups of adjacent to the amino nitrogen atom coalesce; at 323 K two broad signals at δ 3.16 and 4.44 form, at 263 K the methylene protons resolve into four diastereotopic signals at δ 2.88 and 3.44, and δ 4.10 and 4.77.

^g Two methine signals superimpose with other signals

^h The two methylene groups of adjacent to the amino nitrogen atom coalesce; at 323 K two broad signals at δ 3.23 and 4.32 form, at 263 K the methylene protons resolve into four diastereotopic signals at δ 2.90 and 3.55, and δ 4.04 and 4.60.

ⁱ One methylene, two methine and a quaternary signals superimpose with other signals.

^j One methine signal and one quaternary signal superimpose with other signals.

^k Corresponds to [M]⁺ calcd. m/z = 1230.4630.

Acknowledgements

We cordially thank Fonds der Chemischen Industrie and the Deutsche Forschungsgemeinschaft (Mu 1088/9-1) for the financial support.

Supplementary Material

Supporting Information contains general remarks to starting materials and analytics, as well as the ^1H and ^{13}C NMR spectra of compounds **1a** and **8**.

References

1. Shindy, H. A. *Dyes Pigm.* **2017**, *145*, 505–513.
<https://doi.org/10.1016/j.dyepig.2017.06>
2. Panigrahi, M.; Dash, S.; Patel, S.; Mishra, B. K. *Tetrahedron* **2012**, *68*, 781–805.
<https://doi.org/10.1016/j.tet.2011.10.069>
3. Kulinich, A. V.; Ishchenko, A. A. *Russ. Chem. Rev.* **2009**, *78*, 141–164.
<https://doi.org/10.1070/RC2009v078n02ABEH003900>
4. Shirinian, V. Z.; Shimkim, A. A. *Top. Heterocycl. Chem.* **2008**, *14*, 75–105.
https://doi.org/10.1007/7081_2007_110
5. Mishra, A.; Behera, R. K.; Behera, P. K.; Mishra, B. K.; Behera, G. B. *Chem. Rev.* **2000**, *100*, 1973–2011.
<https://doi.org/10.1021/cr990402t>
6. Hamer, F. M. *The Cyanine Dyes and Related Compounds*; Interscience: New York, London, 1964.
<https://doi.org/10.1002/9780470186794>
7. Kim, T.-D.; Lee, K.-S. *Macromol. Rapid Commun.* **2015**, *36*, 943–958.
<https://doi.org/10.1002/marc.201400749>
8. Castet, F.; Rodriguez, V.; Pozzo, J.-L.; Ducasse, L.; Plaquet, A.; Champagne, B. *Acc. Chem. Res.* **2013**, *46*, 2656–2665.
<https://doi.org/10.1021/ar4000955>
9. Marder, S. R. *Chem. Commun.* **2006**, 131–134.
<https://doi.org/10.1039/B512646K>
10. Würthner, F.; Wortmann, R.; Meerholz, K. *ChemPhysChem* **2002**, *3*, 17–31.
[https://doi.org/10.1002/1439-7641\(20020118\)3:1<17::AID-CPHC17>3.0.CO;2-N](https://doi.org/10.1002/1439-7641(20020118)3:1<17::AID-CPHC17>3.0.CO;2-N)
11. For a recent review on dyes and pigments in semiconductor applications, see e.g. Gsänger, M.; Bialas, D.; Huang, L.; Stolte, M.; Würthner, F. *Adv. Mater.* **2016**, *28*, 3615–3645.
<https://doi.org/10.1002/adma.201505440>
12. For an actual review on merocyanines in organic photovoltaics, see Arjona-Esteban, A.; Lenze, M. R.; Meerholz, K.; Würthner, F. In *Elementary Processes in Organic Photovoltaics*, Leo, K., Ed., *Book Series: Advances in Polymer Science*, **2017**, *272*, 193–214.
https://doi.org/10.1007/978-3-319-28338-8_8
13. Würthner, F. *Acc. Chem. Res.* **2016**, *49*, 868–876.
<https://doi.org/10.1021/acs.accounts.6b00042>

14. Heyne, B. *Photochem. Photobiol. Sci.* **2016**, *15*, 1103–1114.
<https://doi.org/10.1039/C6PP00221H>
15. Kovtun, Y. P.; Prostota, Y. O.; Shandura, M. P.; Poronik, Y. M.; Tolmachev, A. I. *Dyes Pigm.* **2004**, *60*, 215–221.
[https://doi.org/10.1016/S0143-7208\(03\)00152-9](https://doi.org/10.1016/S0143-7208(03)00152-9)
16. Kovtun, Y. P.; Prostota, Y. O.; Tolmachev, A. I. *Dyes Pigm.* **2003**, *58*, 83–91.
[https://doi.org/10.1016/S0143-7208\(03\)00038-X](https://doi.org/10.1016/S0143-7208(03)00038-X)
17. Yagi, S.; Maeda, K.; Nakazumi, H. *J. Mater. Chem.* **1999**, *9*, 2991–2997.
<https://doi.org/10.1039/A905098A>
18. Levi, L.; Müller, T. J. J. *Chem. Soc. Rev.* **2016**, *45*, 2825–2846.
<https://doi.org/10.1039/C5CS00805K>
19. *Functional Organic Materials*, Müller, T. J. J.; Bunz, U. H. F., Eds., Wiley-VHC: Weinheim, 2007.
<https://doi.org/10.1002/9783527610266>
20. Levi, L.; Müller, T. J. J. *Eur. J. Org. Chem.* **2016**, 2907–2918.
<https://doi.org/10.1002/ejoc.201600409>
21. *Multi-component Reactions in Organic Synthesis*, Zhu, J.; Wang, Q.; Wang, M.-X., Eds., Wiley-VHC: Weinheim, 2015.
<https://doi.org/10.1002/9783527678174>
22. Müller, T. J. J. In *Science of Synthesis Series: Multicomponent Reactions 1 – General Discussion and Reactions Involving a Carbonyl Compound as Electrophilic Component*, Müller, T. J. J. Ed., Georg Thieme: Stuttgart, Germany, 2014, p 5–27.
<https://doi.org/10.1055/sos-SD-210-00002>
23. D'Souza, D. M.; Müller, T. J. J. *Chem. Soc. Rev.* **2007**, *36*, 1095–1108.
<https://doi.org/10.1039/B608235C>
24. Dömling, A.; Ugi, I. *Angew. Chem. Int. Ed.* **2000**, *39*, 3169–3210.
[https://doi.org/10.1002/1521-3773\(20000915\)39:18<3168::AID-ANIE3168>3.0.CO;2-U](https://doi.org/10.1002/1521-3773(20000915)39:18<3168::AID-ANIE3168>3.0.CO;2-U)
25. D'Souza, D. M.; Kiel, A.; Herten, D. P.; Müller, T. J. J. *Chem. Eur. J.* **2008**, *14*, 529–547.
<https://doi.org/10.1002/chem.200700759>
26. D'Souza, D. M.; Rominger, F.; Müller, T. J. J. *Angew. Chem. Int. Ed.* **2005**, *44*, 153–158.
<https://doi.org/10.1002/anie.200461489>
27. Gers-Panther, C. F.; Müller, T. J. J. In *Advances in Heterocyclic Chemistry: Heterocyclic Chemistry in the 21st Century: A Tribute to Alan Katritzky*, Scriven, E. F. V.; Ramsden, C. A. Eds., **2016**, *120*, 67–98.
<https://doi.org/10.1016/bs.aihch.2016.04.007>
28. Müller, T. J. J. *Drug Discov. Today Technol.* **2018**, *29*, 19–26.
<https://doi.org/10.1016/j.ddtec.2018.06.003>
29. Hong, Y.; Lam, J. W. Y.; Tang, B. Z. *Chem. Commun.* **2009**, 4332–4353.
<https://doi.org/10.1039/B904665H>
30. Hong, Y.; Lam, J. W. Y.; Tang, B. Z. *Chem. Soc. Rev.* **2011**, *40*, 5361–5388.
<https://doi.org/10.1039/C1CS15113D>
31. Hu, R.; Leung, N. L. C.; Tang, B. Z. *Chem. Soc. Rev.* **2014**, *43*, 4494–4562.
<https://doi.org/10.1039/C4CS00044G>
32. For a view on the historical perspective of AIE, see Würthner, F. *Angew. Chem. Int. Ed.* **2020**, *59*, 14192–14196.
<https://doi.org/10.1002/anie.202007525>

33. Merkt, F. K.; Müller, T. J. J. *Isr. J. Chem.* **2018**, *58*, 889–900.
<https://doi.org/10.1002/ijch.201800058>
34. Müller, T. J. J. In *Aggregation Induced Emission: Materials and Applications*, Fujiki, M.; Tang, B. Z.; Liu, B. eds., ACS Symposium Series e-book, **2016**, Chapter 6, pp 85–112.
<https://doi.org/10.1021/bk-2016-1226.ch006>
35. D'Souza, D. M.; Muschelknautz, C.; Rominger, F.; Müller, T. J. J. *Org. Lett.* **2010**, *12*, 3364–3367.
<https://doi.org/10.1021/ol101165m>
36. Muschelknautz, C.; Mayer, B.; Rominger, F.; Müller, T. J. J. *Chem. Heterocycl. Comp.* **2013**, *49*, 922–934.
<https://doi.org/10.1007/s10593-013-1320-3>
37. Denißen, M.; Nirmalanathan, N.; Behnke, T.; Hoffmann, K.; Resch-Genger, U.; Müller, T. J. J. *Mater. Chem. Front.* **2017**, *1*, 2013–2026.
<https://doi.org/10.1039/c7qm00198c>
38. Muschelknautz, C.; Visse, R.; Nordmann, J.; Müller, T. J. J. *Beilstein J. Org. Chem.* **2014**, *10*, 599–612.
<https://doi.org/10.3762/bjoc.10.51>
39. For mechanistic, methodological and photophysical studies on the insertion-alkynylation reaction, see Schönhaber, J.; D'Souza, D. M.; Glißmann, T.; Mayer, B.; Janiak, C.; Rominger, F.; Frank, W.; Müller, T. J. J. *Chem. Eur. J.* **2018**, *24*, 14712–14723.
<https://doi.org/10.1002/chem.201802237>
40. Denißen, M.; Hannen, R.; Itskalov, D.; Biesen, L.; Nirmalanathan-Budau, N.; Hoffmann, K.; Reiss, G. J.; Resch-Genger, U.; Müller, T. J. J. *Chem. Commun.* **2020**, *56*, 7407–7410.
<https://doi.org/10.1039/D0CC03451G>
41. Lu, L.; Lachicotte, R. J.; Penner, T. L.; Perlstein, J.; Whitten, D. G. *J. Am. Chem. Soc.* **1999**, *121*, 8146–8156.
<https://doi.org/10.1021/ja983778h>
42. Würthner, F.; Yao, S.; Beginn, U. *Angew. Chem. Int. Ed.* **2003**, *42*, 3247–3250.
<https://doi.org/10.1002/anie.200351414>
43. Simon, J.; Vacus, J. *Adv. Mater.* **1995**, *7*, 797–800.
<https://doi.org/10.1002/adma.19950070908>
44. Würthner, F.; Thalacker, C.; Diele, S.; Tschierske, C. *Chem. Eur. J.* **2001**, *7*, 2245–2253.
[https://doi.org/10.1002/1521-3765\(20010518\)7:10<2245::AID-CHEM2245>3.0.CO;2-W](https://doi.org/10.1002/1521-3765(20010518)7:10<2245::AID-CHEM2245>3.0.CO;2-W)
45. van Nostrum, C. F. *Adv. Mater.* **1996**, *8*, 1027–1030.
<https://doi.org/10.1002/adma.19960081221>
46. Niedballa, J.; Reiss, G. J.; Müller, T. J. J. *Eur. J. Org. Chem.* **2020**, 5019–5024.
<https://doi.org/10.1002/ejoc.202000823>

This paper is an open access article distributed under the terms of the Creative Commons Attribution (CC BY) license (<http://creativecommons.org/licenses/by/4.0/>)